DOI: 10.1002/anie.201406404

Noble-Gas Compounds

Xenon(II) Polyfluoridotitanates(IV): Synthesis and Structural Characterization of $[Xe_2F_3]^+$ and $[XeF]^+$ Salts**

Kristian Radan, Evgeny Goreshnik, and Boris Žemva**

Dedicated to Professor Hermann-Josef Frohn on the occasion of his 70th birthday

Abstract: *Thermal reaction between XeF_2 and excess TiF_4 resulted in the unexpected formation of a highly ionized Xe^{II} species. The products $[Xe_2F_3][Ti_8F_{33}]$ and $[XeF]_2[Ti_9F_{38}]$ represent the first examples of $[Xe_2F_3]^+$ and $[XeF]^+$ compounds, which differ from known Xe^{II} salts containing discrete fluoride anions with pentavalent metalloid/metal centers. A new structural type of 2D polyanion $[Ti_8F_{33}]^-$ and the formation and structure of the novel 1D $[Ti_9F_{38}]^{2-}$ are discussed. Both products were characterized by single-crystal X-ray analysis and Raman spectroscopy.*

To date, the $[XeF]^+$ and $[Xe_2F_3]^+$ species could only be formed by using the strongest known Lewis acids, such as AsF_5, SbF_5, and BiF_5, in reaction with a moderately strong Lewis base, XeF_2.[1] An alternative route to these compounds is the direct oxidation of elemental xenon using certain metal(VI) hexafluorides (e.g., PtF_6,[2] RhF_6,[3] RuF_6,[4] and IrF_6).[5] Since Bartlett's discovery of noble-gas reactivity in 1962 with the oxidation of Xe by PtF_6,[2] the salts $[XeF][MF_6]$ (M = As,[6,7] Sb,[7] Bi,[7] Ir,[5] and Ru[8]), $[XeF][M_2F_{11}]$ (M = Sb,[7,9,10] Bi[7]), $[Xe_2F_3][MF_6]$ (M = As,[11a,c,12] Sb[12]), and $[XeF][IrSbF_{11}]$[5] have been structurally characterized.

In contrast, the metal tetrafluorides are weaker Lewis acids than the pentafluorides and are not expected to be able to efficiently remove the fluoride ion from XeF_2.[1] The systems XeF_2/MF_4 (M = Ti,[13] Cr,[14,15] Mn,[16] Rh,[3] Pd,[17] Pt,[18] and Sn[19]) were investigated and several phases were isolated, but the X-ray crystal structure has been reported for only two compounds, namely $XeF_2{\cdot}CrF_4$[14] and $XeF_2{\cdot}2\,CrF_4$.[15] In both cases, the measured Xe−F bond lengths indicate that XeF_2 is at the beginning of its ionization pathway ($XeF_2 \rightarrow [XeF]^+ + F^-$),[20] justifying the formulation of the compounds as adducts.

Nevertheless, a suggested quantitative Lewis acidity scale ranks a free gaseous molecule of SnF_4 very high, with a fluoride affinity value close to that of AsF_5 (SnF_4: 98.2 kcal mol^{-1}; AsF_5: 105.9 kcal mol^{-1}).[21] Most of the above-mentioned MF_4 compounds have polymeric structures in the solid state,[22] which is reflected in their relatively high melting points and their low solubility in solvents which are commonly used in noble-gas chemistry, such as anhydrous HF (aHF) or BrF_5.

To overcome the association energies that hinder the fluoride-accepting potential of the MF_4 compounds, gas-phase reactions were carried out in an appropriate temperature range where vapors of the majority of the MF_4 compounds (M = Ti, Cr, Mn, Rh, Pd, Pt, Sn) contain tetrahedral molecules.[22] The reaction temperature should be low enough to prevent the thermal decomposition of products formed and high enough for the MF_4 reagent to be at least partially volatile. Moreover, MF_4 must be resistant to the oxidizing power of molten/gaseous XeF_2 and, at the same time, its oxidation potential has to be low enough to prevent the facile formation of XeF_4. The compound TiF_4 matches these requirements and therefore, after nearly 40 years, it was again employed in reaction with XeF_2.

In a previous study,[13] TiF_4 was thermally treated with excess XeF_2 at 120 °C, yielding the compounds $n\,XeF_2{\cdot}TiF_4$ ($n = 1.5$, 1, 0.5). In the present work, thermal reactions employing a range of different molar ratios of the reactants XeF_2 and TiF_4 were investigated, starting from XeF_2:TiF_4 5:1 to XeF_2:TiF_4 1:5. In a typical run, the temperature of the reaction mixture was held at approximately 135 °C for several hours, above the triple point of XeF_2 (129.03 °C).[23] When the molar ratio exceeded 1:1 in favor of the TiF_4 reagent, crystals of $[Xe_2F_3][Ti_8F_{33}]$ (**1**)[24,31] and $[XeF]_2[Ti_9F_{38}]$ (**2**)[25,31] started to grow on the wall of the reaction tube after approximately 2–3 hours at 135 °C.

In most of the experiments, phases of both **1** and **2** were found and the experimental conditions were subsequently tuned to maximize the yield and the crystallinity of the desired product. The extensive work carried out included variations in the heating and cooling rates, the molar ratios of the starting material, the reaction times, the lengths and type (nickel, quartz, fluoroplastic) of the reactors used, as well as quenching at different temperatures. It was also found that the reaction atmosphere (argon or anhydrous HF) and its pressure have a significant effect on the formation and crystal quality of the products. Moreover, to detect any potential new phase formed, the contents of the reactor tubes were meticulously screened after each run with Raman spectroscopy and special attention was given to classify all of the different morphologies present.

---

[*] K. Radan, Dr. E. Goreshnik, Prof. B. Žemva
Department of Inorganic Chemistry and Technology
"Jožef Stefan" Institute and
Jožef Stefan International Postgraduate School
Jamova 39, 1000 Ljubljana (Slovenia)
E-mail: kristian.radan@ijs.si
boris.zemva@ijs.si

[**] We thank the Slovenian Research Agency (ARRS) for financial support in the form of Research Program P1-0045 (Inorganic Chemistry and Technology) and the Young Researchers Program PR-03723 (K.R.).

Supporting information for this article is available on the WWW under http://dx.doi.org/10.1002/anie.201406404.

Perhaps the most striking feature of compound **1** is the formation of the $[Xe_2F_3]^+$ cation itself. Until now, the crucial requirement for the synthesis and successful isolation of $Ng_2F_3^+$ (Ng = Kr, Xe) species has been to have an excess of the binary Ng^{II} fluoride over the appropriate Lewis acid, and not the contrary. This excess was either ensured by the initial reaction stoichiometry or was provided by the reaction intermediates during their solvolysis in aHF.[12] In the case of the monoclinic species $[Xe_2F_3][AsF_6]$, the compound was also obtained by the thermal decomposition of $[XeF][AsF_6]$ as a result of the volatile nature of the AsF_5.[11a,c]

The geometry of the $[Xe_2F_3]^+$ cation has played an important role in extending hypervalent bond theory to include the 5-center 6-electron bond.[11d] However, relatively little related data is available as only three such salts have been structurally characterized. A single-crystal X-ray diffraction study of **1** revealed that it contained the widest $Xe{-}F_b{-}Xe$ angle among known $[Xe_2F_3]^+$ compounds with a value of 164.3(3)° (previously found to vary from 139.8(8) to 160.3(3)° in trigonal $[Xe_2F_3][AsF_6]$ and $[Xe_2F_3][SbF_6]$, respectively). Experimental evidence for the facile deformation of this angle was confirmed using DFT methods.[12] While a Hartree–Fock study[11d] predicted a linear Xe–F–Xe bridge for the free cation, our result is in perfect agreement with the previous Christiansen–Ermler ECP (effective core potential) calculation,[12] which predicted a nonlinear structure with a $Xe{-}F_b{-}Xe$ angle of 168°.

The extended crystal structure of **1** consists of alternating anion and cation layers parallel to the *ab*-plane (Figures S1 and S2 in the Supporting Information). Although the polymeric anion with the formulation $[Ti_8F_{33}]^-$ has already been found in the compound $CsTi_8F_{33}$,[26] the substitution of spherical Cs^+ with the planar V-shaped $[Xe_2F_3]^+$ cations leads to a dramatic change in its structure. A basic structural motif in **1** (Figure 1) resembles a recently reported isolated cubic $[Ti_8F_{36}]^{4-}$ anion[27] comprising eight TiF_6 octahedra (Figure S3). Such octameric units in **1** are connected through six shared fluoride vertices—four roughly along the crystallographic *b*-axis and two along the *a*-axis, forming a complex polyanion layer. The $[Xe_2F_3]^+$ cations are trapped in semi-closed channels which form as a result of indentations between the anion layers (Figure S4). The $[Xe_2F_3]^+$ cation provides 12 long Xe···F contacts to the anion layers (from 3.047(3) to 3.601(3) Å) lying within the sum of the Xe and F van der Waals radii[28] (3.63 Å) to the anion layers and two more interactions (3.177(4) Å, 3.528(4) Å) with the neighboring cations (Figure S5). The Raman spectrum of **1** (Figure 2) is dominated by the band detected at 594 cm^{-1}, which is in the characteristic $Xe{-}F_t$ stretch region (ca. 575–600 cm^{-1}) for $[Xe_2F_3]^+$ salts.[11,12]

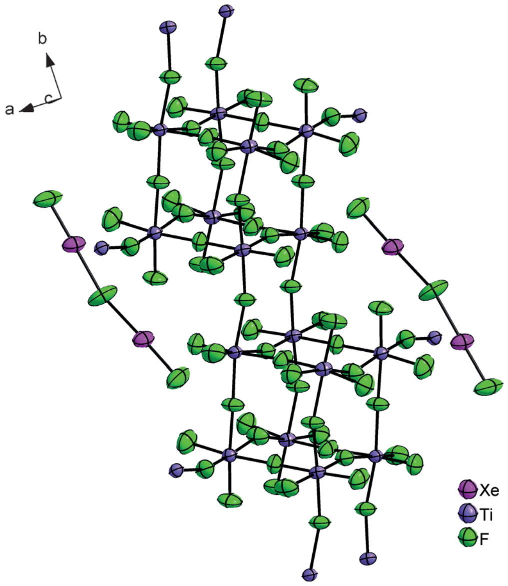

Figure 1. Selected structural fragment of the product $[Xe_2F_3][Ti_8F_{33}]$. Ellipsoids are set at 50% probability.

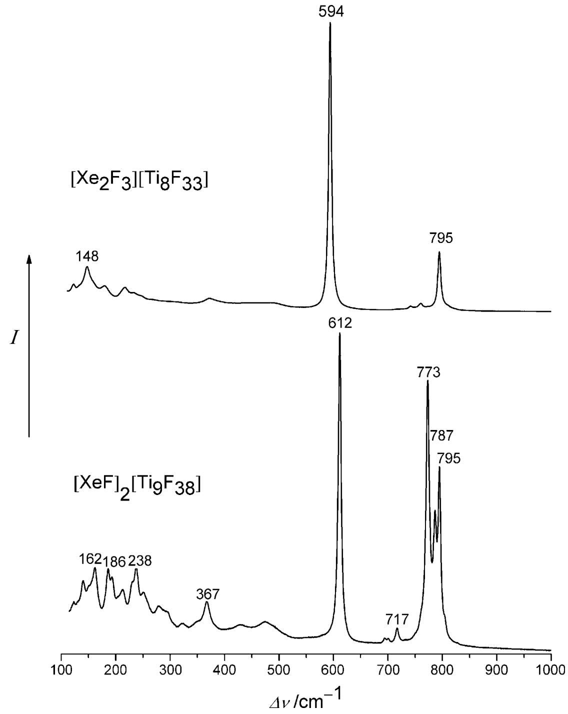

Figure 2. Raman spectra of powdered samples of **1** (top) and **2** (bottom).

Interestingly, the crystal structure of compound **2** (Figure S6) resembles the solid-state structure of TiF_4[29] itself. The structure of TiF_4 consists of Ti_3F_{15} building blocks, where three TiF_6 octahedra share two *cis* vertices. These trimeric rings are then connected through fluorine atoms, generating isolated columns in an infinite array (Figure S7).[29] In **2**, the incorporation of linear XeF_2 molecules into the crystal lattice resulted in the association of trimeric rings to form trigonal prismatic Ti_9F_{39} units, which are linked together through single fluorine bridges along the *c*-axis, as shown in Figure 3. In this way, the newly formed 1D polyanion $[Ti_9F_{38}]^{2-}$ preserves the columnar structure found in TiF_4 and with nine Ti atoms/unit, it has the largest associations among established polymeric fluoridotitanates(IV). In order for the Ti atoms to adopt the given structure and maintain the octahedral coordination, two F atoms need to be extracted from a F^- donor molecule. This is achieved by the interaction

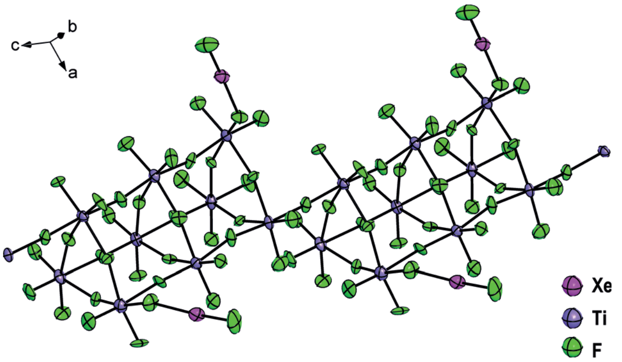

Figure 3. The molecular structure of $[XeF]_2[Ti_9F_{38}]$ (**2**) showing a selected part of the columnar packing structure. Ellipsoids are set at 50% probability.

of two XeF_2 ligands by means of Xe$-F_b-$Ti bridges ($F_b =$ bridging fluorine atom), with the Ti atoms lying on the face diagonal (parallel to the *ac*-plane) of each Ti_9F_{39} block (Figure 3).

The Xe$-F_t$ ($F_t =$ terminal fluorine atom) and Xe$-F_b$ bond lengths in **2** are comparable with the $[XeF]^+$ salts of the strongest Lewis acids (Table 1). Additional interactions between the $[(Ti_9F_{38})^{2-}]_\infty$ columns arise from the secondary coordination spheres of two crystallographically independent Xe atoms, where several Xe···F contacts with distances ranging from 3.024(4) to 3.628(5) Å were identified (Figure S9). Further evidence for the high degree of XeF_2 ionization is given by the vibrational spectrum, where a sharp band assigned to the Xe$-F_t$ stretching frequency can be found at 612 cm^{-1} (Figure 2).

To our knowledge, both isolated compounds **1** and **2** are the first reported Xe^{II} salts containing fluoride anions of higher dimensionality. For the salts of other cations, Raman spectroscopy proved to be especially helpful to distinguish between the various fluoridotitanate species, where it was found that the frequencies of the most intense Raman bands, belonging to the symmetric in-phase Ti$-F_t$ stretching mode, increased with increasing TiF_4 content and decreasing anion charge.[30] Such a ready identification of the anion nature is further facilitated by a recent report,[27] where the calculated *x*/*n* ratios ($x =$ total anion charge, $n =$ number of TiF_6 octahedra present in the anion) for several compounds containing $[Ti_nF_{4n+x}]^{x-}$ anions were correlated with their measured Raman frequencies. Herein, the observed strong bands at 773 cm^{-1} for $[Ti_9F_{38}]^{2-}$ ($x/n = 0.22$) and 795 cm^{-1} in the case of $[Ti_8F_{33}]^-$ ($x/n = 0.125$), which can be assigned to the symmetric in-phase Ti$-F_t$ stretching modes, clearly follow the trend described previously, thus additionally supporting the relationship between the partial charges on the TiF_6 octahedra and the corresponding Raman shifts.

Table 1: Xe$-F_t$ and Xe$-F_b$ bond lengths and Xe$-F_t$ vibrational frequencies among selected $[XeF]^+$ salts and compound **2**.

Compound	Xe$-F_t$ [Å]	Xe$-F_b$ [Å]	T [K][a]	$\Delta\nu$ [cm^{-1}][b]
$[XeF][AsF_6]$[c]	1.888(3)	2.208(3)	100	607(96) 611(100)
$[XeF][SbF_6]$[c]	1.885(2)	2.278(2)	100	616(100) 621(66)
$[XeF][Sb_2F_{11}]$[c]	1.888(4)	2.343(4)	100	621(100)[e]
$[XeF][IrF_6]$[d]	1.854(4) 1.854(5) 1.867(5)	2.220(4) 2.245(5) 2.272(4)	133	602(60)[e] 608(44)[e]
$[XeF][BiF_6]$[c]	1.913(7)	2.204(7)	100	602(48) 608(11)
$[XeF]_2[Ti_9F_{38}]$ (**2**)	1.890(5) 1.882(4)	2.245(4) 2.219(4)	150	612(100)

[a] Temperature at which the X-ray data was collected. [b] Values in parentheses denote relative intensities. [c] See Ref. [7]. Raman spectra recorded at 110 K. [d] See Ref. [5]. [e] See Ref. [11b]. Raman spectra recorded at room temperature unless otherwise stated.

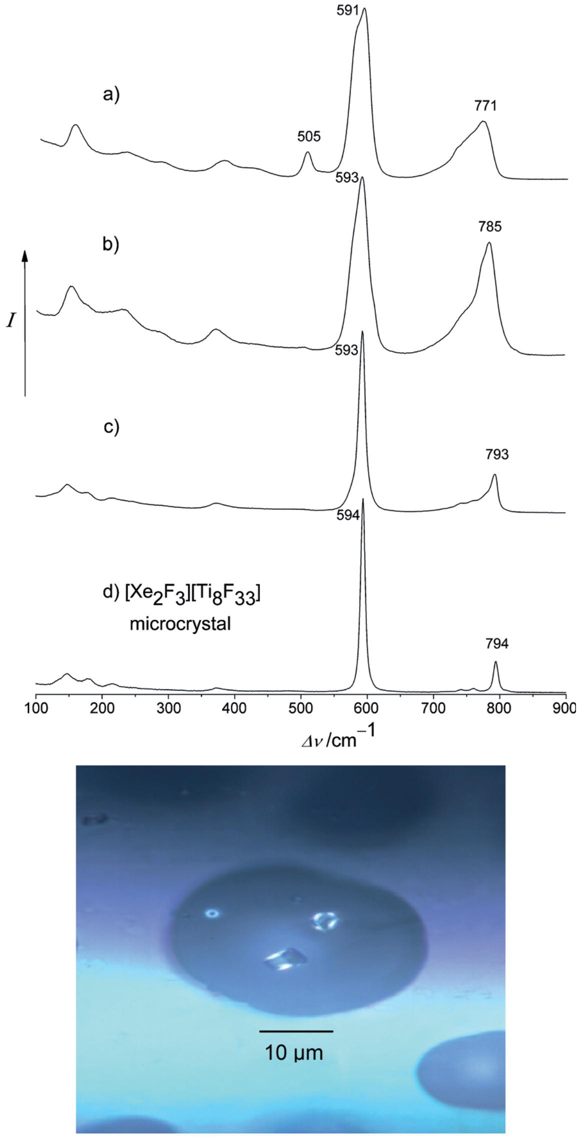

Figure 4. Top: The crystallogenesis of compound **1** followed by Raman spectroscopy, showing the gradual transition from the glassy material of unknown composition (a) to the microcrystals (d), formed on the wall of a sealed quartz capillary used for the melting-point determination. Although the contents were extensively screened, no trace of compound **2** was detected. Bottom: Image showing the crystal seeds of **1** growing on the capillary wall inside clear spherical regions of the glassy matrix.

In almost all experiments, the formation of an amorphous gel-like product was observed at the beginning of the heating process. This material solidifies to form a glassy product upon cooling to room temperature, and does not give any XRD pattern. Its Raman spectrum (Figure 4 a–c) features a broad band between 550 and 620 cm^{-1}, indicating multiple Xe–F modes of a complex composition or more likely of a mixture of compounds. An attempt to determine the melting interval of this material provided us unexpectedly with a remarkable insight into the early stage of the crystallization process. A precise Raman study of the partially molten matrix obtained after thermal treatment (up to 142 °C), demonstrates unambiguously that microscopic crystal seeds of compound **1** (Figure 4 bottom, Figure S10) are formed first. Figure 4 (top) shows a gradual decomposition of the glassy material as a function of the distance from the crystal seeds of product **1**. The wavenumber shift from 771 cm^{-1}, through 785 cm^{-1} to 794 cm^{-1}, indicative of the increasing ordering of molecules to form larger polyanion associations and/or of a decrease of the anion charge, is consistent with a slight increase in the XeF_2 ionization. The increase in XeF_2 ionization is best represented by the change in the $Xe{-}F_t$ stretch frequency which is shifted and sharpened from a broad 591 cm^{-1} band of the glassy material to a 594 cm^{-1} peak obtained on microcrystals of **1**. The synthetic pathways leading to the formation of product **2** probably involve either direct formation from the glassy solid after the formation of **1** has left a deficiency of available XeF_2 molecules, or an equimolar gas-phase reaction of **1** with TiF_4, affording crystals of **2**. The proposed reaction routes are in agreement with the visual (morphology-based) observations and spectroscopic results. These results were obtained by carefully following the experimental runs, thus witnessing the formation and accumulation of compound **2** during prolonged exposure to high temperatures (approximately 130 °C) or when using higher molar ratios of TiF_4. A further investigation of this system is currently underway to decipher the intriguing reaction mechanism and to clarify the initial role and composition of the glassy product.

Experimental Section

Caution: XeF_2 must be handled in a well-ventilated hood, and protective clothing must be worn at all times by the experimentalist, who should be familiar with this compound and the hazards associated with it.

Several experiments were carried out to improve the yield and selectivity of the reactions and the crystallinity of the desired products and the optimized procedure is described below. Each poly(tetrafluoroethylene-co-hexafluoropropylene) (FEP) reaction vessel was vacuum dried and passivated overnight with elemental fluorine at 1.3 bar prior to use. Further details relating to the crystal-structure determination and the Raman spectroscopy are provided in the Supporting Information.

1: A FEP reaction vessel (tubing, 6 mm internal diameter, 8 mm external diameter), equipped with a PTFE (polytetrafluoroethylene) valve, was filled with TiF_4 (23 mg, 0.19 mmol) and XeF_2 (16 mg, 0.09 mmol) in a glove box (argon atmosphere, $[H_2O] < 0.5$ ppm). The reaction vessel assembly, including contents, were then evacuated at −196 °C on a vacuum line and the FEP tube was sealed. The sealed reaction tube was then heated to 135 °C for 12 hours. Initially, the mixture turned into a pale-yellow gel-like material, which began to slowly decompose during the heating process. Careful cooling to 110 °C (2 °C h^{-1}) afforded colorless, rod-like crystals (Figure S11), which were isolated from the reaction vessel and immersed in perfluorinated oil (ABCR, AB102850, 98 %, perfluorodecalin, *cis* and *trans*) in the glove box. A suitable crystal was selected at low temperature (−15 °C) under the microscope and transferred into the cold nitrogen stream of the X-ray diffractometer.

2: The same procedure was used for the synthesis, crystallization, and isolation as detailed for **1**. The thermal reaction between TiF_4 (32 mg, 0.26 mmol) and XeF_2 (15 mg, 0.09 mmol) afforded colorless prismatic crystals (Figure S11) of compound **2**.

Received: June 20, 2014
Revised: August 24, 2014
Published online: October 14, 2014

Keywords: fluorine · hypervalent compounds · Lewis acids · structure elucidation · xenon

---

[1] a) H. Selig, J. H. Holloway, *Top. Curr. Chem.* **1984**, *124*, 33 – 90; b) B. Žemva, *Croat. Chem. Acta* **1988**, *61*, 163 – 187; c) G. J. Schrobilgen in *Encyclopedia of Physical Science and Technology, Vol. 10* (Ed.: M. F. Hawthorne), *3rd ed.*, Academic Press, San Diego, **2002**, pp. 449 – 461; d) M. Tramšek, B. Žemva, *Acta Chim. Slov.* **2006**, *53*, 105 – 116; e) G. J. Schrobilgen, M. D. Moran in *Kirk-Othmer Encyclopedia of Chemical Technology, 5th ed.*, Wiley, Hoboken, **2006**, pp. 323 – 343; f) D. S. Brock, G. J. Schrobilgen, B. Žemva in *Comprehensive Inorganic Chemistry, Vol. 1* (Eds.: J. Reedijk, K. Poeppelmeier), Elsevier, Oxford, **2013**, pp. 755 – 822.
[2] N. Bartlett, *Proc. Chem. Soc.* **1962**, *6*, 218.
[3] N. Barlett, N. K. Jha in *Noble Gas Compounds*, (Ed.: H. H. Hyman), University of Chicago Press, Chicago, **1963**, p. 23.
[4] C. L. Chernick, H. H. Claassen, R. R. Fields, H. H. Hyman, J. G. Malm, W. M. Manning, M. S. Matheson, L. A. Quarterman, F. Schreiner, H. Selig, I. Sheft, S. Siegel, E. N. Sloth, L. Stein, M. H. Studier, J. L. Weeks, M. H. Zirkin, *Science* **1962**, *138*, 136 – 138.
[5] F. Tamadon, S. Seidel, K. Seppelt, *Acta Chim. Slov.* **2013**, *60*, 491 – 494.
[6] A. Zalkin, D. L. Ward, R. N. Biagioni, D. H. Templeton, N. Bartlett, *Inorg. Chem.* **1978**, *17*, 1318 – 1322.
[7] H. S. A. Elliott, J. F. Lehmann, H. P. A. Mercier, H. D. B. Jenkins, G. J. Schrobilgen, *Inorg. Chem.* **2010**, *49*, 8504 – 8523.
[8] N. Bartlett, M. Gennis, D. D. Gibler, B. K. Morrell, A. Zalkin, *Inorg. Chem.* **1973**, *12*, 1717 – 1721.
[9] V. M. McRae, R. D. Peacock, D. R. Russell, *Chem. Commun.* **1969**, 62 – 63.
[10] J. Burgess, C. J. W. Fraser, V. M. McRae, R. D. Peacock, D. R. Russell, *J. Inorg. Nucl. Chem.* **1976**, *28*, 183 – 188.
[11] a) F. O. Sladky, P. A. Bullinger, N. Bartlett, B. G. DeBoer, A. Zalkin, *Chem. Commun.* **1968**, 1048 – 1049; b) F. O. Sladky, P. A. Bulliner, N. Bartlett, *J. Chem. Soc. A* **1969**, 2179 – 2188; c) N. Bartlett, B. G. DeBoer, F. J. Hollander, F. O. Sladky, D. H. Templeton, A. Zalkin, *Inorg. Chem.* **1974**, *13*, 780 – 785; d) D. A. Dixon, A. J. Arduengo III, W. B. Farnham, *Inorg. Chem.* **1989**, *28*, 4589 – 4593.
[12] B. A. Fir, M. Gerken, B. E. Pointner, H. P. A. Mercier, D. A. Dixon, G. J. Schrobilgen, *J. Fluorine Chem.* **2000**, *105*, 159 – 167.
[13] B. Žemva, J. Slivnik, M. Bohinc, *J. Inorg. Nucl. Chem.* **1976**, *38*, 73 – 74.
[14] K. Lutar, I. Leban, T. Ogrin, B. Žemva, *Eur. J. Solid State Inorg. Chem.* **1992**, *29*, 713 – 727.
[15] K. Lutar, H. Borrmann, B. Žemva, *Inorg. Chem.* **1998**, *37*, 3002 – 3006.

[16] a) B. Žemva, J. Zupan, J. Slivnik, *J. Inorg. Nucl. Chem.* **1971**, *33*, 3953–3955; b) M. Bohinc, J. Grannec, J. Slivnik, B. Žemva, *J. Inorg. Nucl. Chem.* **1976**, *38*, 75–76.

[17] N. Bartlett, B. Žemva, L. Graham, *J. Fluorine Chem.* **1976**, *7*, 301–320.

[18] L. Graham, O. Graudejus, N. K. Jha, N. Bartlett, *Coord. Chem. Rev.* **2000**, *197*, 321–334.

[19] B. Družina, B. Žemva, *J. Fluorine Chem.* **1986**, *34*, 233–239.

[20] B. Žemva, A. Jesih, D. H. Templeton, A. Zalkin, A. K. Cheetham, N. Bartlett, *J. Am. Chem. Soc.* **1987**, *109*, 7420–7427.

[21] K. O. Christe, D. A. Dixon, D. McLemore, W. W. Wilson, J. A. Sheehy, J. A. Boatz, *J. Fluorine Chem.* **2000**, *101*, 151–153.

[22] a) D. Babel in *Structure and Bonding*, *Vol. 3*, (Eds.: C. K. Jørgensen, J. B. Neilands, R. S. Nyholm, D. Reinen, R. J. P. Williams), Springer, Berlin and New York, **1967**, pp. 30–32; b) C. E. Housecroft, A. G. Sharpe, *Inorganic Chemistry*, *3th ed.*, Pearson, Essex, **2008**, p. 544.

[23] F. Schreiner, G. N. McDonald, C. L. Chernick, *J. Phys. Chem.* **1968**, *72*, 1162–1166.

[24] Crystal data for **1**: colorless crystal, $M_r = 1329.54$, monoclinic space group $P2/a$, $a = 17.6347(5)$, $b = 8.4106(2)$, $c = 19.9028(5)$ Å, $\beta = 97.1399(10)°$, $V = 2929.06(13)$ Å^3, $Z = 4$, $\rho_{\mathrm{calcd}} = 3.016\ \mathrm{g\,cm^{-3}}$, $F(000) = 2432$, $T = 150$ K; 23246 reflections up to $\theta = 29°$ collected, thereof 5574 with $I > 2\sigma(I)$, 6602 independent reflections, 416 parameters. Final R indices: $R_1 = 0.063$ (all), $wR_2 = 0.1549$ (all). The final difference Fourier synthesis gave min/max residual electron density of $-1.98/2.18\ \mathrm{e\,Å^{-3}}$.

[25] Crystal data for **2**: colorless prism, $M_r = 1453.7$, monoclinic space group Cc, $a = 17.5967(8)$, $b = 15.3862(6)$, $c = 11.9529(6)$ Å, $\beta = 108.2795(16)°$, $V = 3072.9(2)$ Å^3, $Z = 4$, $\rho_{\mathrm{calcd}} = 3.142\ \mathrm{g\,cm^{-3}}$, $F(000) = 2664$, $T = 150$ K; 12054 reflections up to $\theta = 29°$ collected, thereof 6345 with $I > 2\sigma(I)$, 6712 independent reflections, 461 parameters. Final R indices: $R_1 = 0.037$ (all), $wR_2 = 0.086$ (all). The final difference Fourier synthesis gave min/max residual electron density of $-1.39/1.09\ \mathrm{e\,Å^{-3}}$.

[26] H. Bialowons, B. G. Müller, *Z. Anorg. Allg. Chem.* **1995**, *621*, 1223–1226.

[27] I. M. Shlyapnikov, E. A. Goreshnik, Z. Mazej, *Chem. Commun.* **2013**, *49*, 2703–2705.

[28] A. J. Bondi, *J. Phys. Chem.* **1964**, *68*, 441–451.

[29] H. Bialowons, M. Müller, B. G. Müller, *Z. Anorg. Allg. Chem.* **1995**, *621*, 1227–1231.

[30] K. O. Christe, C. J. Schack, *Inorg. Chem.* **1977**, *16*, 353–359.

[31] The supplementary crystallographic data for this paper may be obtained from the Fachinformationszentrum Karlsruhe, 76344 Eggenstein-Leopoldshafen, Germany (fax: (+49) 7247-808-666; e-mail: crysdata@fiz-karlsruhe.de), on quoting the depository numbers CSD-427949 for $[Xe_2F_3][Ti_8F_{33}]$ or CSD-427950 for $[XeF]_2[Ti_9F_{38}]$.